Article

Cell Chemical Biology

Biosynthetic Pathway Connects Cryptic Ribosomally Synthesized Posttranslationally Modified Peptide Genes with Pyrroloquinoline Alkaloids

Highlights

- Pyrroloquinoline alkaloid biosynthesis is driven by cryptic conserved genes
- Heterologous expression confirms the ammosamide gene cluster
- Ribosomal peptide biosynthesis genes are required for an unprecedented biosynthesis

Authors

Peter A. Jordan, Bradley S. Moore

Correspondence

bsmoore@ucsd.edu

In Brief

Ribosomally synthesized, posttranslationally modified peptides (RiPPs) comprise a vast array of potent, bioactive natural products. Now, Jordan and Moore have connected a collection of conserved cryptic RiPP genes to biosynthesis of lymphostin and the ammosamides, characteristic members of the entire class of pyrroloquinoline alkaloids the biosynthesis of which was previously unknown.

Jordan & Moore, 2016, Cell Chemical Biology *23*, 1504–1514
December 22, 2016
http://dx.doi.org/10.1016/j.chembiol.2016.10.009

CellPress

Please cite this article as: Jordan and Moore, Biosynthetic Pathway Connects Cryptic Ribosomally Synthesized Posttranslationally Modified Peptide Genes with Pyrroloquinoline Alkaloids, Cell Chemical Biology (2016), http://dx.doi.org/10.1016/j.chembiol.2016.10.009

Biosynthetic Pathway Connects Cryptic Ribosomally Synthesized Posttranslationally Modified Peptide Genes with Pyrroloquinoline Alkaloids

Peter A. Jordan[1] and Bradley S. Moore[1,2,3,*]
[1]Scripps Institution of Oceanography, University of California, San Diego, La Jolla, CA 92037, USA
[2]Skaggs School of Pharmacy and Pharmaceutical Sciences, University of California, San Diego, La Jolla, CA 92093, USA
[3]Lead Contact
*Correspondence: bsmoore@ucsd.edu
http://dx.doi.org/10.1016/j.chembiol.2016.10.009

SUMMARY

In an era where natural product biosynthetic gene clusters can be rapidly identified from sequenced genomes, it is unusual for the biosynthesis of an entire natural product class to remain unknown. Yet, the genetic determinates for pyrroloquinoline alkaloid biosynthesis have remained obscure despite their abundance and deceptive structural simplicity. In this work, we have identified the biosynthetic gene cluster for ammosamides A-C, pyrroloquinoline alkaloids from *Streptomyces* sp. CNR-698. Through direct cloning, heterologous expression and gene deletions we have validated the ammosamide biosynthetic gene cluster and demonstrated that these seemingly simple molecules are derived from a surprisingly complex set of biosynthetic genes that are also found in the biosynthesis of lymphostin, a structurally related pyrroloquinoline alkaloid from *Salinispora* and *Streptomyces*. Our results implicate a conserved set of genes driving pyrroloquinoline biosynthesis that consist of genes frequently associated with ribosomal peptide natural product biosynthesis, and whose exact biochemical role remains enigmatic.

INTRODUCTION

Microbial genome sequencing and genome mining have revealed a much greater capacity for secondary metabolite biosynthesis within the genomes of microbial organisms (Bentley et al., 2002; Udwary et al., 2007; Weber, 2014; Zarins-Tutt et al., 2015; Ziemert et al., 2016). This latent capacity is often encoded within so-called orphaned gene clusters for which the chemical product has not been identified. Yet, for many of these orphaned biosynthetic gene clusters (BGCs), gross structure predictions are possible in the absence of chemical information, especially for the most well-characterized biosynthetic systems, such as polyketides, and non-ribosomal and ribosomal peptides (Boddy, 2014). Although such classes of molecules continue to yield important drug leads, special attention has recently been given to non-canonical BGCs, where structure-defining features cannot be predicted solely from sequence information (Cimermancic et al., 2014). Much how the discovery and biochemical characterization of assembly-line biosynthesis has led to the genome mining revolution (Challis, 2008; Corre and Challis, 2009; Walsh and Fischbach, 2010), deciphering the biosynthetic logic of non-canonical biosynthetic pathways will not only yield novel natural products and biochemistry, but also "inform" the bioinformatic tools of future genome mining endeavors.

Alkaloids bearing a pyrrolo[4,3,2-de]quinoline core have been the subject of numerous natural product discovery and total synthesis programs for decades because of their potent biological activity and unique structural features (Figure 1) (Antunes et al., 2005). The vast majority of these molecules have been isolated from marine sponges (over 80 examples), which have traditionally been intractable to genetic tools and laboratory cultivation. Consequently, aside from predictions that the pyrroloquinoline core is derived from tryptophan (Hu et al., 2011), the genes for pyrroloquinoline biosynthesis have not been identified. In 2011, we verified the role of tryptophan in lymphostin biosynthesis and reported on the end-stage biosynthetic events leading to the production of lymphostin in three sequenced strains of the genus *Salinispora* (Miyanaga et al., 2011). In that work, the O-methylation and two-carbon malonyl extension were attributed to the *S*-adenosyl-methionine (SAM)-dependent methyltransferase LymB and the hybrid non-ribosomal peptide synthetase (NRPS)-polyketide synthase LymA, respectively. But there was no indication that neighboring genes at the *lym* genetic locus were responsible for the production of the pyrroloquinoline core.

Besides the *Salinispora*-derived lymphostins, only one other example of bacterial pyrroloquinoline alkaloids has been described. In 2009, Fenical and co-workers reported the isolation and characterization of ammosamides A (**1**) and B (**2**) from the marine bacterium *Streptomyces* sp. CNR-698 (Hughes et al., 2009). As the ammosamides share the same core structural features of lymphostin (Figure 1), they provide a unique opportunity to explore pyrroloquinoline alkaloid biosynthesis in a distinct genomic context. Herein we show that the marine bacteria-derived pyrroloquinoline alkaloids lymphostin and the ammosamides are derived from a highly non-canonical biosynthetic pathway that more closely resembles the genetic features of ribosomally synthesized, posttranslationally modified peptide (RiPP) natural products (Arnison et al., 2013).

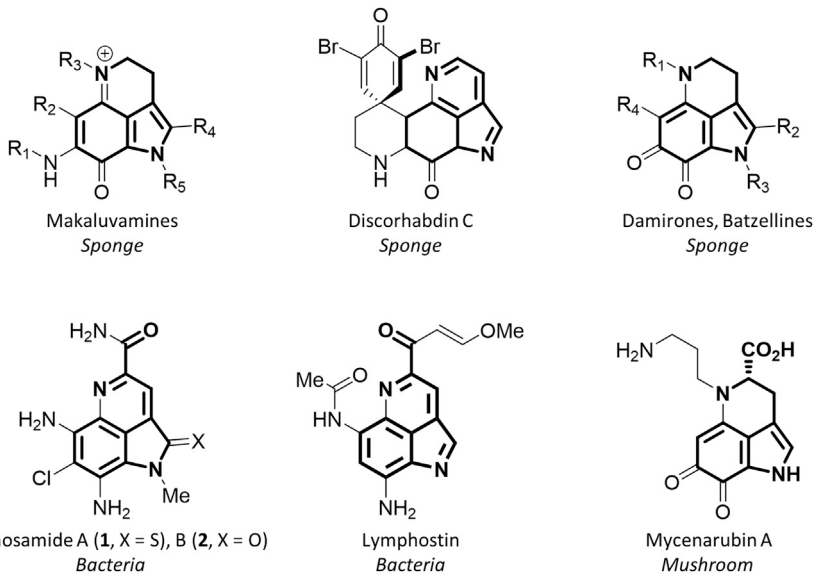

Figure 1. Pyrroloquinoline Alkaloids are Diverse Natural Products Derived from Varied Sources

The pyrrolo[4,3,2-de]quinoline core predicted to be derived from tryptophan is indicated in bold.

RESULTS AND DISCUSSION

Identification of the Ammosamide, *amm*, BGC: Features of Ribosomal Peptide Biosynthesis

The sequenced and assembled genome of *Streptomyces* sp. CNR-698 (GenBank: GCA_000515055.1) was acquired from the Joint Genome Institute. Due to a lack of genetic markers for pyrroloquinoline alkaloid biosynthesis, we were drawn to the chloro-substitution on the ammosamides as a means to identify the *amm* genetic locus in CNR-698. Enzymatic halogenation is often a hallmark secondary metabolism, and having previously established the role of tryptophan in lymphostin biosynthesis, we searched for homologs of the flavin adenine dinucleotide (FAD)-dependent tryptophan halogenase RebH (Yeh et al., 2005) in the CNR-698 draft genome. Indeed, a BLAST (Altschul et al., 1990; Boratyn et al., 2013) search revealed a single genomic scaffold carrying a tryptophan halogenase homolog (*amm3*, Figure 2). We further identified a SAM-dependent methyltransferase (*amm23*) 30 kb downstream of *amm3*, which we suspected could be responsible for the N-methylation on the ammosamides.

Sandwiched between the flavin-dependent halogenase (*amm3*) and SAM-dependent methyltransferase (*amm23*) genes are a collection 20 predicted open reading frames (ORFs), 14 of which are highly conserved based upon sequence identity and overall gene organization to ORFs of unknown function found upstream of the *lymAB* genetic locus in *Salinispora* (Figure 2A, see Table 1 for a complete list of predicted gene functions). Notably, the peripheral ORFs putatively responsible for ammosamide-specific modifications (Figure 2B), including halogenation (*amm3*), oxidation (*amm4*), and methylation (*amm23*), flank a core set of ORFs shared between the two BGCs. Strikingly, these ORFs include four lantibiotic dehydratases (LD) and two peptidases, genes traditionally associated with RiPP biosynthesis. RiPP BGCs, on the other hand, typically harbor just one or two LDs, as in the case of class II–IV systems and class I systems, respectively (Chatterjee et al., 2005). When we queried the Conserved Domain Architecture Retrieval Tool (Geer et al., 2002), it was revealed that each of the *amm* LDs are truncated, lacking both a C-terminal cyclase domain that is typical of class II–IV LDs and a SpaB_C domain that is common among class I LanB systems (LanBs are typically accompanied by stand-alone LanC cyclases). Furthermore, in the few cases where truncated LanBs lack a SpaB_C domain, as in the case of thiopeptide biosynthesis, a stand-alone SpaB_C-like protein is found within the gene cluster. However, we did not observe SpaB or LanC cyclase homologs in the *amm* gene cluster (Zhang et al., 2012) (Li and Kelly, 2010). Despite vague features relating the *amm* and *lym* LDs to lanthipeptide and thiopeptide biosynthesis, the *lym* and *amm* LDs appear to be members of a larger group of small LanBs, many of which have no known function (Ortega et al., 2015).

Included at the beginning of the large conserved biosynthetic operon for *amm* is a short ORF (*amm6*) (Figure 2C) that encodes a peptide bearing a C-terminal tryptophan residue and bears a striking resemblance to RiPP precursor peptides. RiPP biosynthesis often begins with a short peptide sequence consisting of two domains: an N-terminal ''leader'' sequence that bears recognition elements for posttranslational modification, and a ''core'' peptide sequence that is posttranslationally modified prior to proteolytic removal of the leader peptide. Not only is *amm6*, including the C-terminal tryptophan residue, highly conserved among all producers of lymphostin and the ammosamides, but *amm6* and its lymphostin counterpart also contain a conserved ''FNLD'' amino acid motif (FDLD for *lym* and *amm*), which are common leader peptide recognition elements among class I lantibiotics (Chatterjee et al., 2005; van der Meer et al., 1994). Despite the similarities to lanthipeptide biosynthesis, no cysteine residues are present in either of the predicted precursor peptides from the *amm* or *lym* pathways. Cysteine residues are often highly suggestive of posttranslational modifications involving sequential serine and threonine dehydration events, followed by cyclization with cysteine to form thioether bridges, a common feature of lanthipeptide biosynthesis (Arnison et al., 2013). The potential for such chemistry is evidently absent from ammosamide biosynthesis.

Transformation-Associated Recombination Cloning and Heterologous Expression of *amm*: Ammosamide C is the Dominant Pathway Product

To validate whether the *amm* biosynthetic locus is indeed involved in the construction of the ammosamides and to probe the function of key genes, we directly captured the *amm* BGC (see Table 1) by transformation-associated recombination

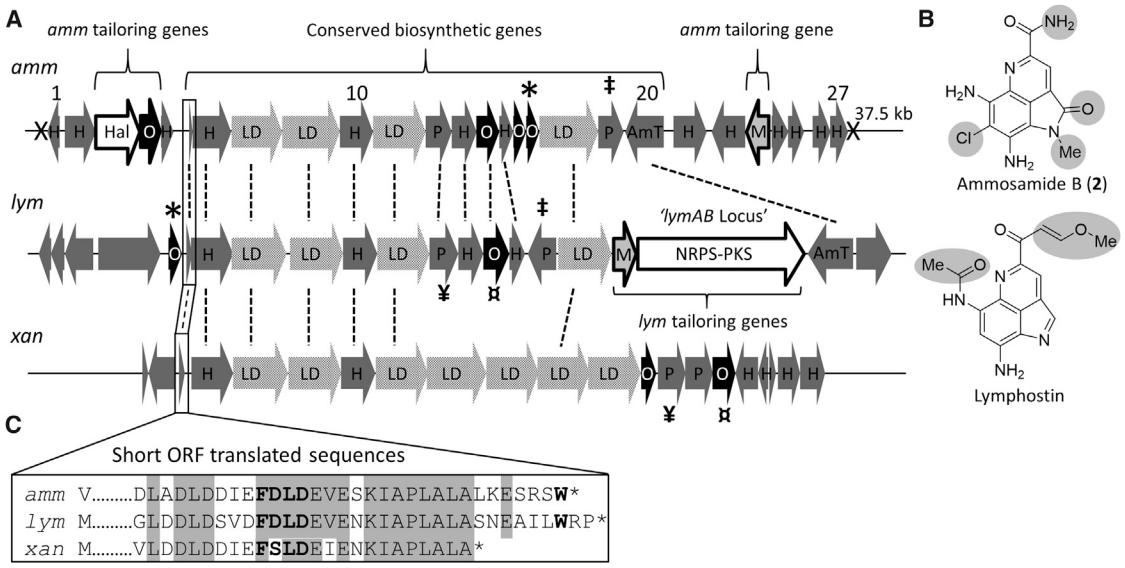

Figure 2. The Ammosamide Biosynthetic Gene Cluster Shares High Gene Sequence Homology and Gene Organization with the BGC for Lymphostin, a Related Natural Product

(A) Alignment of the ammosamide (*amm*) and lymphostin (*lym*) biosynthetic gene clusters. A related orphaned gene cluster (*xan*) from *S. xanthophaeus* is also included. ORFs of high sequence homology are connected with a dotted line. TAR cloning sites for *amm* are indicated with an "X." Conserved genes are indicated with brackets and tailoring genes are outline in black.

(B) For ammosamide B and lymphostin, structural features derived from tailoring genes in their respective pathways are highlighted in gray.

(C) Aligned translated sequences of the short ORFs in *amm*, *lym*, and *xan* pathways. FNLD motif is indicated in bold.

H, hypothetical protein; LD, lantibiotic dehydratase; P, peptidase; O, oxidoreductase; Amt, amidotransferase; M, methyltransferase; Hal, halogenase. Pairs of ‡ * ¤ ¥ indicate homologs.

(TAR) in yeast (Yamanaka et al., 2014). The resulting TAR-assembled "pCAP01/*amm*" vector was transferred to *Escherichia coli* followed by conjugation and chromosomal integration into *Streptomyces coelicolor* M512 (Gomez-Escribano and Bibb, 2012, 2014). Cultures of *S. coelicolor* M512-pCAP01/*amm* yielded ammosamides A and B (Figure 3) with 3- to 4-fold higher production (17 mg each) than the native producer, CNR-698 (Hughes et al., 2009). After only 2 days of growth, we further observed the production of large quantities of ammosamide C (**3**), the reduced precursor to A and B. Although ammosamide C is only a minor component of ethyl acetate extracts from 12 day cultures, the liquid chromatography-mass spectrometry (LC-MS) analysis of aqueous aliquots from both pCAP01/*amm* and CNR-698 cultures revealed that ammosamide C is the predominant product of the *amm* pathway (Figure S1). Furthermore, up to 134 mg/L of ammosamide C can be isolated from 4 day cultures of pCAP01/*amm*. We also observed that large quantities of ammosamide C persists for 1–2 days prior to the formation of either ammosamide A or B. The sluggish final oxidative step suggested that it may proceed under non-enzymatic conditions. Previous work by MacMillan and co-workers showing that a wide range of amidine derivatives of the ammosamides can be generated from ammosamide C supports our observation (Pan et al., 2013).

Gene Deletions of *amm4* and *amm23*: N-Methylation and Oxidative Primary Amide Synthesis are Late-Stage Modifications to the Pyrroloquinoline Core

Despite evidence suggesting a non-enzymatic final oxidation, it was tempting to speculate that the predicted coenzyme F420-dependent oxidase (*amm4*), which is unique to the *amm* BGC, could be responsible for accelerating the final oxidation step. However, upon deletion of *amm4*, extracts of M512-pCAP01/*amm*Δ*amm4* showed no signs of ammosamides A-C. We instead identified and characterized a new highly polar shunt product, ammosamaic acid **4**, that bears a carboxylic acid moiety (Figure 3), implicating *amm4* in primary amide biosynthesis. Typically, oxidative primary amide bond formation involves copper-dependent peptidylglycine-α-amidating monooxygenases (Kulathila et al., 1999; Merkler et al., 1999; Prigge et al., 1997; Silakowski et al., 1999). However, such chemistry is not documented for F420-dependent oxidases, where the 5-deazaflavin co-factor is a functional equivalent of nicotinamide (Walsh, 1986). Although many actinobacteria have the capacity for F420 biosynthesis (Selengut and Haft, 2010), there are limited examples of coenzyme F420 in secondary metabolism (Greening et al., 2016), with the most notable being its role in the final reductive step in oxytetracycline biosynthesis (Wang et al., 2013).

The production of **4** by M512-pCAP01/*amm*Δ*amm4* implies a secondary amide precursor resembling **5** (Figure 3B), such that in the absence of *amm4* a competing hydrolysis is required to yield **4**. However, under no circumstances could we identify precursors such as **5** in extracts of the wild-type or mutant strains. The absence of methylated products in extracts of pCAP01/*amm*Δ*amm4* suggested that N-methylation by *amm23*, a predicted SAM-dependent methyltransferase, takes place after the formation of the primary amide. To test this hypothesis, we inactivated *amm23* and evaluated the methyltransferase

Table 1. Predicted Function of ORFs in the amm Locus of *Streptomyces* sp. CNR-698

Name	Predicted Function	Size (Amino Acids)	Predicted Function of Closest Homolog	% ID	Notes
amm1	(2Fe-2S)-binding protein	157	**HP**, *Streptomyces* sp. CNT-302	98	
amm2	**HP**	486	**HP**, *Amycolatopsis japonica*	55	
amm3	tryptophan halogenase (FAD)	695	*Microbispora carollina*, tryptophan-5-halogenase	60	microbisporicin
amm4	F420 oxidase	146	*Amycolatopsis thermoflava*, F420 Oxidase	42	
amm5	**HP**	199	**HP**, *Streptomyces aurantiacus*	68	
amm6	**HP**	56	**HP**, *Salinispora*, multispecies	68	lymphostin
amm7	**HP**	614	**HP**, *Salinispora*, multispecies	55	lymphostin
amm8	**LD**	806	**LD**, *Salinispora*, multispecies	54	lymphostin
amm9	**LD**	913	**LD**, *Salinispora*, multispecies	61	lymphostin
amm10	**HP**	524	**HP**, *Salinispora*, multispecies	42	lymphostin
amm11	**LD**	832	**LD**, *Salinispora*, multispecies	51	lymphostin
amm12	**P**	419	**P**, *Salinispora*, multispecies	46	lymphostin
amm13	**HP**	393	**HP**, *Salinispora*, multispecies	39	lymphostin
amm14	FAD-dependent oxidase	363	*Salinispora*, multispecies, FAD-dep oxidase	55	lymphostin
amm15	**HP**	225	**HP**, *Salinispora*, multispecies	73	lymphostin
amm16	flavoprotein	199	*Salinispora*, multispecies, flavoprotein	54	
amm17	flavoprotein	212	*Salinispora*, multispecies, flavin reductase	54	lymphostin
amm18	**LD**	936	**LD**, *Salinispora* multispecies	48	lymphostin
amm19	**P** (M20 dipeptidase)	395	**P** (M20 dipeptidase), *Salinispora*, multispecies	62	lymphostin
amm20	asparagine synthase	612	*Salinispora*, multispecies, asparagine synthase	61	lymphostin
amm21	**T**	526	**T**, *Kibdelosporangium* sp. MJ126-NF4	57	
amm22	**HP**	525	**HP**, *Nocardia vinacea*	43	
amm23	**MT**	356	**MT**, *Nocardiopsis* sp. NRRL B-16309	45	
amm24	TetR regulator	201	TetR, *Nocardia brevicatena*	56	
amm25	**HP**	254	*Saccharothrix* sp. NRRL B-16348, glyoxalase	50	
amm26	**HP**	284	**HP**, *Streptomyces* sp. CNT-302	99	
amm27	**HP**	131	**HP**, *Streptomyces* sp. CNT-302	99	

ORFs captured by TAR are named *amm1-27*. For homologs of amm ORFs that are associated with other reported BGCs, the corresponding natural product is indicated in the "Notes" column. NC, not captured; HP, hypothetical protein; LD, lantibiotic dehydratase; P, peptidase; MT, methyltransferase; T, transporter.

knockout mutant M512-pCAP01/*amm*Δ*amm23*, which yielded two new desmethyl ammosamide analogs **6** and **7**.

Overall, heterologous expression of pCAP01/*amm* and the subsequent gene knockouts support the final biosynthetic steps described in Figure 3B, where amide bond formation followed by methylation are preludes to the final non-enzymatic oxidation step. Under all circumstances, only halogenated products could be isolated from M512-pCAP01/*amm* and various mutants, suggesting that chlorination occurs at an earlier stage in the biosynthesis.

Genetic Manipulations of *amm3*: A Flavin-Dependent Tryptophan Halogenase Related to MibH, a RiPP Pathway Halogenase

In consideration of the shared genetic features of the respective *lym* and *amm* gene clusters (Figure 2), we hypothesized that the halogenase Amm3 chlorinates tryptophan or an advanced pyrroloquinoline intermediate, such that deletion mutants might yield non-halogenated products (Zehner et al., 2005). Deletion of *amm3* abolished production of the ammosamides and any related pyrroloquinoline intermediates (Figure 3A). This observation is consistent with known $FADH_2$-dependent tryptophan halogenases that have been biochemically characterized, where halogenation of free tryptophan is often the beginning of biosynthesis, and chemical complementation of tryptophan halogenase knockouts can rescue production (Zeng and Zhan, 2011). However, cultures of M512-pCAP01/*amm*Δ*amm3* could not be rescued when supplemented with 6-chlorotryptophan (Figure S2). Only when genetically complemented with pKY01/*amm3* under the control of the constitutively active promotor *ermE* could ammosamide production be restored (Figure 3A) (Yamanaka et al., 2012). Genetic complementation also yielded compound **4** as the dominant product, suggesting that gene deletion of *amm3* may have disrupted the expression of the downstream oxidase *amm4*. Incidentally, larger-scale cultures of M512-pCAP01/*amm*Δ*amm3* + pKY01/*amm3* also provided **8**, a presumed byproduct of ambient oxidation of **4**.

A closer bioinformatics analysis revealed that *amm3* is unusual among characterized $FADH_2$-dependent halogenases, which

Please cite this article as: Jordan and Moore, Biosynthetic Pathway Connects Cryptic Ribosomally Synthesized Posttranslationally Modified Peptide Genes with Pyrroloquinoline Alkaloids, Cell Chemical Biology (2016), http://dx.doi.org/10.1016/j.chembiol.2016.10.009

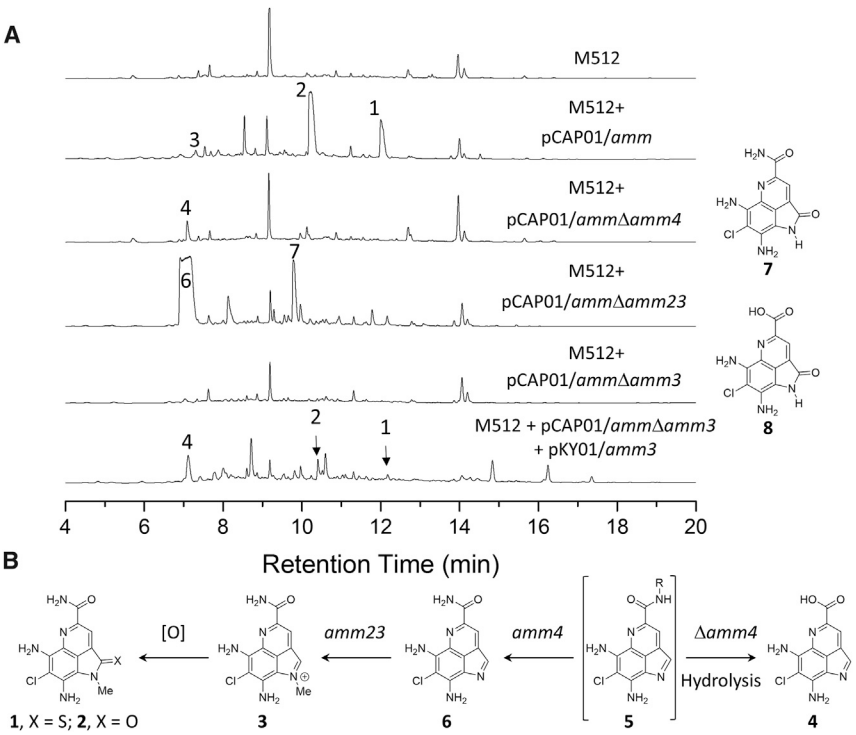

Figure 3. Targeted Gene Deletions Reveal the Final Stages of Ammosamide Biosynthesis, Yielding Four New Metabolites

(A) LC-MS analysis of *S. coelicolor* M512 mutants integrated with pCAP01/*amm* and gene-deleted mutated vectors. Chromatograms at 254 nm are provided above. Peaks for ammosamides A (**1**), B (**2**), and C (**3**) and shunt products are indicated with compound numbers.

(B) Proposed biosynthetic scheme for the final stages of the ammosamide biosynthesis. Compounds **7** and **8** are oxidized analogs of **4** and **6**, respectively, and are thought to arise from ambient oxidation as their production is culture scale- and extraction condition-dependent. Compound **5** was not identified, but is implied based on this biosynthetic scheme. Peaks were verified by retention time with respect to a positive control (pCAP01/*amm*), UV absorbance, and mass spectrometry.

typically fall into two categories; those that utilize free substrates and those that utilize an acyl carrier protein (ACP)-bound substrate. However, the *amm* BGC lacks any ORF resembling an ACP gene. The closest homolog of Amm3 based upon sequence identity (61%) is MibH, a tryptophan-5-halogenase involved in the biosynthesis of microbisporicin, a RiPP-class peptide antibiotic from *Microbispora carollina* (Foulston and Bibb, 2010). Phylogenetic analysis shows that Amm3 and MibH are distinct from all other flavin-dependent halogenases (Figure 4). Given that microbisporicin is a RiPP product, and the strict limitations of aminoacyl-tRNA substrates available for ribosomal peptide biosynthesis, tryptophan halogenation via MibH is posttranslational. The implication that Amm3 similarly chlorinates a peptide substrate is intriguing.

Genetic Manipulations of Conserved Biosynthetic Genes: RiPP-Related ORFs are Essential for Ammosamide Production

The presence of four putative LDs (*amm8*, *-9*, *-11*, and *-18*) in the *amm* cluster is further suggestive that ammosamide may be derived from a peptide precursor. Individual in-frame gene deletions of all four LDs in the *amm* pathway resulted in the complete loss of production of the ammosamides and any detectable shunt products (Figure S3), supporting the role of LDs in ammosamide biosynthesis. Similarly, deletion of each of the conserved flavin-dependent oxidoreductase genes (*amm14*, *-16*, and *-17*), the peptidase *amm19*, and one of the four hypothetical genes (*amm7*) resulted in a complete loss of ammosamide production (Figure S3). The absence of detectable shunt products from these mutants suggests their involvement in the requisite oxidative steps to convert peptidic tryptophan to the ammosamides.

Genetic Manipulations of *amm6*: A Short ORF Encoding a 56-Amino Acid Peptide Is Essential for Biosynthesis

Having established the necessity of RiPP-related genes in the *amm* pathway, we were particularly interested in the predicted 56-amino acid peptide encoded by *amm6*. Based upon the conserved C-terminal tryptophan and leader peptide recognition elements (Figure 2C), we imagined a scenario where the encoded peptide delivers a C-terminal tryptophan residue for posttranslational modification by pathway enzymes. Deletion of *amm6* and consequent loss of ammosamide production support its role for biosynthesis (Figure 5). With an *amm6* knockout mutant in hand, we next set out to probe the requirement of the conserved C-terminal tryptophan residue by attempting to genetically complement M512-pCAP01/*amm*Δ*amm6* with plasmids carrying *amm6* mutants where the tryptophan residue had been replaced. However, ammosamide production could not be restored even with a positive control of native *amm6* (Figure 5). Upon closer examination, we identified a region of DNA downstream of *amm6* encompassing the 5′ end of *amm7* that includes a large inverted repeat with a predicted RNA secondary structure (ΔG = −57.7 kcal/mol). Such RNA secondary structures are described in lanthipeptide pathways and putatively serve to control the stoichiometry of the precursor peptide relative to downstream modifying enzymes (Foulston and Bibb, 2010; McAuliffe et al., 2001).

To preserve the implicit relationship between *amm6* and *amm7* while still placing the expression of both genes under the control of the *ermE* promotor, we cloned *amm6-amm7* from a single PCR product into the pKY01 vector. Integration of pKY01/*amm6amm7* into the pCAP01/*amm*Δ*amm*6 mutant restored ammosamide production (Figure 5). However, variants of pKY01/*amm6amm7* where the terminal tryptophan was removed (pKY01/*amm6*(W56stp)*amm7*) or mutated to a cysteine residue (pKY01/*amm6*(W56C)*amm7*) also restored production of the ammosamides (Figure 5). This experiment demonstrated that the C-terminal tryptophan residue is not a strict requirement for

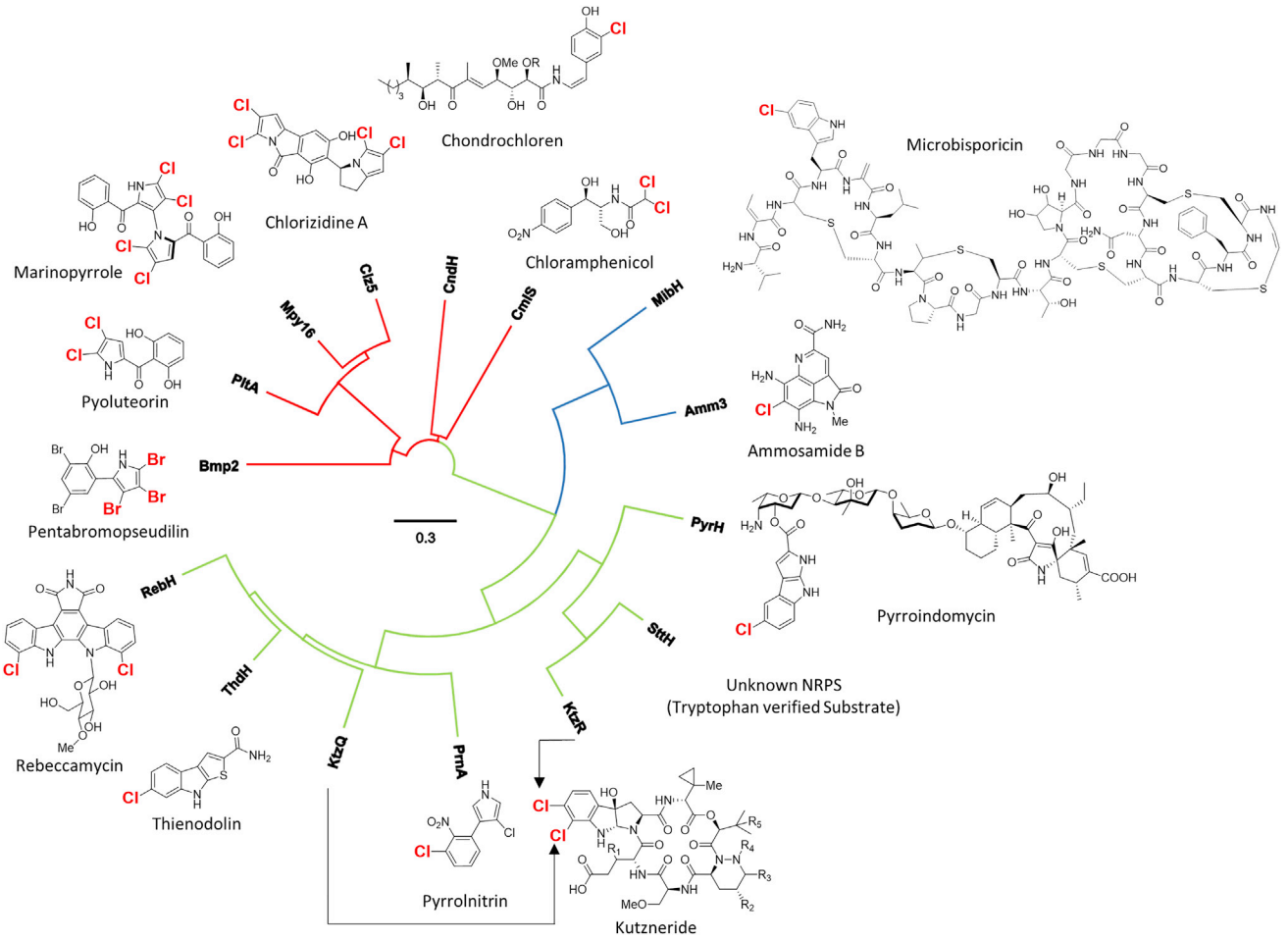

Figure 4. Neighbor-Joining Tree of Flavin-Dependent Halogenases Associated with Characterized Secondary Metabolites

On each of the corresponding secondary metabolites, the site of halogenation is indicated. Red branches correspond to halogenases that modify acyl carrier protein-bound substrates, and green branches correspond to enzymes that halogenate free substrates. The blue branch is occupied by Amm3, described in this work, and MibH, a halogenase that likely modifies a tryptophan embedded in a peptide substrate. Multiple sequence comparison by log-expectation alignment and phylogenetic tree were generated using Geneious 8.1.5.

ammosamide biosynthesis and thereby not the source of its pyrroloquinoline core structure. In contrast, integration of pKY01/*amm7* alone into the pCAP01/*amm*Δ*amm6* mutant did not restore production, verifying that the genetic complementation with pKY01/*amm6amm7*, or related tryptophan-substituted constructs, were not simply a result of overexpressing functional *amm7*.

These results raise the question: How does a highly conserved, but not strictly necessary, tryptophan residue relate to a predicted precursor peptide sequence that appears to play an essential role in the biosynthesis? Several examples in the literature offer clues to how this may work. It is a common feature of RiPP biosynthesis that substrate recognition, via the leader peptide recognition elements, is spatially segregated from catalysis for peptide-modifying enzymes (Koehnke et al., 2015; Oman and van der Donk, 2010). Consequently, there are a growing number of examples of RiPP pathway enzymes where the leader sequence need not be connected to the core peptide sequence, and *trans* activation of the modifying enzyme by the discrete leader peptide drives product formation (Goto et al., 2014; Khusainov and Kuipers, 2012; Oman et al., 2012). Whether the peptide product of *amm6*, lacking a tryptophan residue, is similarly able to *trans* activate *amm* pathway enzymes, which in turn utilize the cellular pool of free tryptophan, is the subject of ongoing in vitro biochemical investigations.

Orphaned BGCs Bearing Features of the *amm* and *lym* Pathways

The *lym* and *amm* pathways are highly unusual with several distinct genetic features that enable the identification of either pathway, as well as potentially related pathways, through similarity searches and genome mining tools such as antiSMASH 3.0 (Weber et al., 2015). We have identified homologs of Amm6 from Gram-positive and -negative bacteria that all share a highly conserved amino acid sequence toward the C terminus (Figure S4A). However, in many cases, the Amm6 homologs are missing the final seven to nine amino acids, which include the conserved tryptophan, which is a common feature of the *lym*

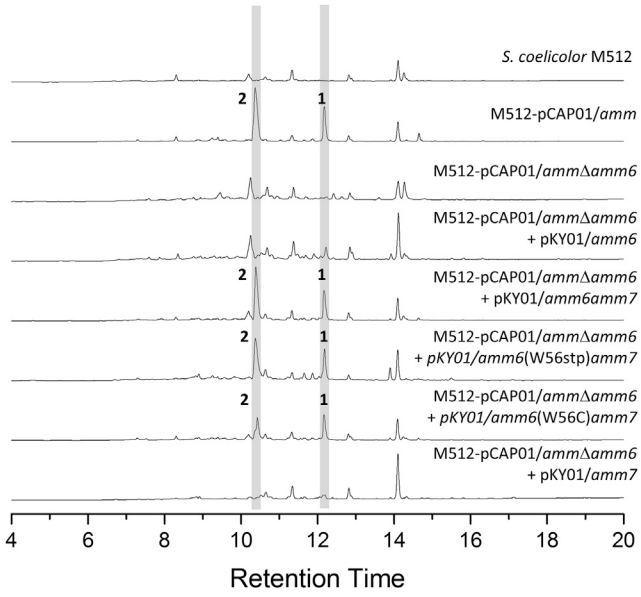

Figure 5. Gene Deletion of *amm6* and Genetic Complementation of pCAP01/*amm*Δ*amm6* with Various pKY01 Constructs

pKY01 is an integrative plasmid for the expression of gene products under the control of a the *ermE* promotor. Peaks for ammosamides A (**1**) and B (**2**) produced by *S. coelicolor*-M512 pCAP01/*amm* are indicated. The absence of ammosamide A and B was verified by retention time with respect to the positive control (pCAP01/*amm*), UV absorbance, and mass spectrometry. Related metabolites could not be identified by UV absorbance or extracting masses.

and *amm* gene clusters. Rather, the truncated Amm6 homologs are often associated with other BGCs apparently unrelated to *lym* or *amm*. Scant evidence exists for how these Amm6 homologs relate to BGCs in their genetic neighborhood. However, recent studies with *Myxococcus xanthus* point to an *amm6* homolog, MXAN_1609, which is found upstream of an NRPS gene cluster (MXAN_1608-1598), and is regulated by MXAN4899, a bacterial enhancer binding protein responsible for regulating the production of multiple secondary metabolites (Volz et al., 2012).

With regard to the remainder of the *amm* gene cluster, we have identified an orphaned BGC similar to *amm* and *lym* from *Streptomyces xanthophaeus* NRRL B-3004, a terrestrial bacterium not known to produce pyrroloquinoline type molecules. The "*xan*" cluster maintains the same gene order and identity of the ORFs comprising the beginning of the shared *lym* and *amm* biosynthetic ORFs, including a short ORF encoding a peptide similar to *amm6*, which bears an "FNLD" leader peptide motif, but lacks a C-terminal tryptophan residue (Figure 2C, for a complete list of *xan* ORFs see Table S1). In addition to the four LDs found in the *amm* and *lym* clusters, the *xan* cluster features three additional predicted LDs. Although one or two LDs are a requirement for lanthipeptide biosynthesis, the presence of multiple LDs is atypical, further underscoring the obscurity of these BGCs. Other gene clusters encompassing multiple, clustered LDs include two predicted lanthipeptide pathways from *Bacillus halodurans* C-125 and *Desmospora* sp. 8437, each of which contain up to seven LDs (Figure S4). As in the *amm*, *lym*, and *xan* pathways, the LDs associated with the *Bacillus* and *Desmospora* pathways are also truncated, lacking both a C-terminal cyclase domain and a SpaB_C domain. Incidentally, the orphaned lanthipeptide pathway from *B. halodurans* also includes a short ORF encoding a peptide with high sequence homology to the *lym*, *amm*, and *xan* pathways (Figure S4). Too little is known about these predicted lanthipeptide biosyntheses and if or how their respective biosynthetic products relate to pyrroloquinoline alkaloids, such as lymphostin and the ammosamides.

In summary, we have identified the ammosamide BGC (*amm*) in *Streptomyces* sp. CNR-698, which bears a striking resemblance to the biosynthetic pathway for the closely related pyrroloquinoline alkaloid, lymphostin. Our analysis points to a conserved set of ORFs of unknown function that are responsible for pyrroloquinoline core biosynthesis in each pathway. Through direct cloning and heterologous expression of the *amm* pathway, and targeted gene deletions of *amm* tailoring genes, we reconstructed the final stages of ammosamide biosynthesis and provided four new ammosamide analogs. These results also revealed several rare biosynthetic features, including a predicted F420-dependent oxidase involved in primary amide biosynthesis and an unusual tryptophan halogenase phylogenetically related to a flavin-dependent halogenase involved in RiPP natural product biosynthesis. Perhaps most surprising, the genes shared between the *amm* and *lym* pathways consist of genes normally associated with RiPP natural product biosynthesis, including four predicted LDs and a short ORF encoding a putative RiPP pathway precursor peptide. Through targeted gene deletions of all four *amm*-associated LDs and the gene (*amm*6) encoding the putative precursor peptide, we have established their requirement for biosynthesis. However, it remains unclear whether the peptide encoded by *amm6* supplies a substrate for posttranslational modification, or modulates the activity of pathway enzymes.

SIGNIFICANCE

The *lym* and *amm* pathways are unlike any biosynthetic gene clusters described to date, exemplifying the genetic diversity that drives small-molecule biosynthesis. Although the *lym* and *amm* pathways currently represent only two examples of an unprecedented biosynthesis, the connection of lymphostin and the ammosamides to the broader class of pyrroloquinoline alkaloids is intriguing. Likely, many more opportunities to explore the biosynthesis of pyrroloquinoline alkaloids will come from marine sponges, which are the dominant source of these natural products (Antunes et al., 2005**). But, like many sponge-derived natural products, the pyrroloquinolines may be products of symbiotically associated bacteria, the genetic information of which is increasingly becoming accessible through metagenomic sequencing (**Hentschel et al., 2012**). Insights from bacterial pyrroloquinoline biosynthesis may enlighten a general paradigm for the assembly of many pyrroloquinoline alkaloids, enabling future studies of sponge-derived pyrroloquinolines and further expanding our basic understanding of the chemical diversity afforded through unconventional biosynthetic pathways.**

EXPERIMENTAL PROCEDURES

General

General methods including chemical and biological reagents and instrumentation employed in these studies can be found in the online Supplemental Experimental Procedures.

Direct Capture of the *amm* Gene Cluster using Transformation-Associated Recombination

To directly capture the 37.5-kb region encompassing the ammosamide (*amm*) BGC, we followed the general procedure described by Yamanaka et al. (2014). Details specific to the TAR capture vector for the *amm* BGC can be found in the online Supplemental Experimental Procedures.

Genetic Manipulations of pCAP01/*amm*

All genetic manipulations of pCAP01/*amm* were carried out using λ Red recombination-mediated PCR-targeted gene deletion, as described by Gust et al. (2003). Individual gene disruption cassettes (for *amm3*, *-4*, *-7*, *-8*, *-9*, *-11*, *-14*, *-16*, *-17 -18*, *-19*, and *-23*) were generated via PCR amplification of the apramycin resistance cassette (*aac(3)IV*) with flanking FRT sites from pMXT19 (Tang et al., 2015). Primers were designed with 39 nucleotides matching the adjacent sequences of the targeted gene. Gene replacement by λ Red recombination was achieved in *E. coli* BW25113/pKD20 carrying the pCAP01/*amm* construct. Mutated pCAP01/*amm* constructs were confirmed by restriction digest (NcoI) and PCR and then transferred to *E. coli* BT340 for flippase (FLP) recombinase-mediated excision of the apramycin resistance gene. The corresponding knockouts, with FLP scar were verified by restriction digest and sequencing prior to transfer into *S. coelicolor* M512.

Gene deletion of *amm6* was carried out in a similar manner as that described in Yamanaka et al. (2012). An *aac(3)IV* cassette was amplified from pIJ773 by PCR using primers containing two NdeI (CATATG) restriction sites directly adjacent to the 39 nucleotides matching the region flanking *amm6*, such that the introduction of CATATG preserves the start codon of *amm7* for in-frame gene replacement. Replacement of *amm6* as described above was achieved in *E. coli* BW25113/pKD20 carrying pCAP01/*amm*. Excision of the apramycin resistance cassette from the mutant plasmid by NdeI digestion, followed by gel purification and ligation, yielded pCAP01/*ammΔamm6*.

Integration of Wild-Type and Mutant pCAP01/*amm* in *S. coelicolor* M512

Included in the pCAP01 vector backbone are the φC31 integrase gene (*int*) and the corresponding attachment site (*attP*) for integration into *S. coelicolor*. pCAP01/*amm* and mutant variants were introduced to *E. coli* ET12567 by electroporation and transferred to *S. coelicolor* M512 by triparental conjugation facilitated by *E. coli* ET-12567/pUB307. Kanamycin (Kan)-resistant colonies were grown until sporulation on mannitol soy flour (MS) agar, with Kan and nalidixic acid (Nal), then plated for a second round of selection on Kan and Nal MS agar plates. Colonies of M512 with chromosomal insertion of pCAP01/*amm* were verified by PCR (gDNA isolated from 5-day tryptic soy broth [TSB] cultures). Exconjugants were screened using primer pairs corresponding to the sites of gene deletion and the resulting PCR product validated by Sanger sequencing. Spore stocks, which were used for all subsequent cultures, were created from a third round of selection on Kan-Nal MS agar plates. For each mutant, three to four individual colonies were selected for secondary metabolite profiling.

General Method for Genetic Complementation

The pKY01 plasmid, an integrative plasmid with *ermE* promotor and apramycin resistance cassette, was used for genetic complementation experiments, as described previously (Yamanaka et al., 2012). pKY01 constructs were created using either Gibson Cloning or by traditional cloning using the NdeI and HindIII restriction sites of pKY01. The assembled plasmids were validated by restriction digestion and sequence prior to transfer to *E. coli* ET-12567 for triparental conjugation into designated *S. coelicolor* M512-pCAP01/*amm* mutants (see above). Exconjugants were selected on MS agar with apramycin (Apra) and Nal, and the colonies allowed to grow to sporulation twice. Primers F-pKY01Sc and R-pKY01Sc were used for screening exconjugants from isolated gDNA and Sanger sequencing of the corresponding PCR product. Spore stocks, which were used for all subsequent cultures, were created from a third round of selection on Kan-Nal MS agar plates. For each mutant, three to four individual colonies were selected for secondary metabolite profiling.

Design of pKY01/*amm6amm7* Mutants Used for Genetic Complementation

Due to the overlapping *amm6* tryptophan codon (TGG) and *amm7* start codon (ATG), we were limited to mutations converting tryptophan to either a stop codon (W56stp) or a cysteine (W56C) residue. These mutants are depicted as "pKY01/*amm6*(W56stp)*amm7*" and "pKY01/*amm6*(W56C)*amm7*" in this article. As a consequence of *amm6-amm7* overlap, mutating the tryptophan codon to a stop codon (TGG→TGA) also converts a valine residue on *amm7* to leucine. Similarly, mutating the tryptophan codon to a cysteine codon (TGG→TGC) converts the valine residue on *amm7* to methionine. These perturbations do not appear to affect the outcome of the experiments.

Secondary Metabolite Profiling of *S. coelicolor* M512-pCAP01/*amm* and Mutants

Cultures of *S. coelicolor* M512-pCAP01/*amm* and mutant strains were started from 20 μL of spores germinated in 200 μL of 2× YT (yeast extract, tryptone) then added to 3 mL of TSB with Nal and Kan. TSB precultures were grown for 5–7 days at 30°C, prior to using 0.3 mL to inoculate 15 mL of R5 production medium without antibiotics (Kieser et al., 2000). Production cultures were grown for 12 days at 30°C and analyzed using the following method: cultures were centrifuged to pellet M512 cells and the resulting supernatant loaded onto a 1 g C18 solid-phase extraction column that was washed, conditioned, and pre-equilibrated at 5% acetonitrile (MeCN). The column was then washed with 6 column volumes of the 5% high-performance liquid chromatography (HPLC)-grade acetonitrile to remove salts and polar compounds, and then the entire column flushed with 9 column volumes of 85% MeCN. The eluted contents were frozen and the solvent was removed by lyophilization. The lyophilized residue was then dissolved in 0.4 mL of HPLC-grade MeOH and analyzed by LC-MS using a Phenomenex Kinetex 2.6 μm XB-C18 100 Å, 150 × 4.6 mm column (0–3 min isocratic 10% MeCN, 3–23 min 10%–100% MeCN; mobile phase buffered with 0.1% formic acid).

Secondary Metabolite Profiling of *S. coelicolor* M512-pCAP01/*ammΔamm6*

Cultures of *S. coelicolor* M512-pCAP01/*ammΔamm6*, including those genetically complemented with pKY01 constructs, were started from 20 μL of spores germinated in 200 μL of 2× YT then added to 3 mL of TSB with Nal and Apra. TSB precultures were grown for 5–7 days at 30°C prior to using 1 mL to inoculate 50 mL of R5 medium without antibiotics. Cultures were grown for 12 days then extracted 3 times with 50 mL of ethyl acetate and concentrated. The resulting residue was dissolved in 50 μL of DMSO then diluted with 450 μL of MeCN. This solution was filtered through a 50 μL plug of C18 silica to remove lipophilic components followed by 500 μL of MeCN. The eluate was then analyzed by LC-MS using a Phenomenex Kinetex 2.6 μm XB-C18 100 Å, 150 × 4.6 mm column (0–3 min isocratic 10% MeCN, 3–23 min 10%–100% MeCN; mobile phase buffered with 0.1% formic acid).

Time Course of Production of Ammosamides A-C

Cultures of *S. coelicolor* M512-pCAP01/*amm* in R5 medium or *Streptomyces* sp. CNR-698 in A1 were sampled daily starting 1 day following inoculation from TSB preculture or A1 preculture, respectively. Aliquots were diluted with an equal volume of HPLC-grade MeOH, and the 1:1 mixtures were vortexed for 1 min then centrifuged at maximum speed for 5 min on a benchtop centrifuge. The supernatant was then filtered through a 0.2 μm filter and analyzed by LC-MS using a Phenomenex Luna 5 μm C18(2) 100 Å, 100 × 4.6 mm column (0–3 min isocratic 10% MeCN, 2–10 min 10%–100% MeCN, 10–12 min 100% MeCN; mobile phase buffered with 0.1% formic acid).

Chemical Complementation of M512-pCAP01/*ammΔamm3*

Secondary metabolite profiling for chemical complementation experiments was performed as above, with R5 medium supplemented with 6-chloro-D,L-tryptophan. R5 medium solutions were prepared by adding 6-chloro-D,L-tryptophan (Chem-Impex International, Cat. 20931) or L-tryptophan (control) to

a final concentration of 4 mM, prior to autoclave sterilization. The R5 medium was then used as described above for secondary metabolite profiling. Production cultures were extracted using C18 solid-phase extraction and analyzed by LC-MS using a Phenomenex Kinetex 2.6 μm XB-C18 100 Å, 150 × 4.6 mm column (0–3 min isocratic 10% MeCN, 3–23 min 10%–100% MeCN; mobile phase buffered with 0.1% formic acid).

Production and Isolation of Ammosamide C from M512-pCAP01/*amm*

A 50 mL culture of R5 medium was inoculated with 1 mL of preculture of M512-pCAP01/amm (5 days, TSB medium) and allowed to grow for 4 days prior to liquid extraction with *n*-butanol (3× 50 mL). The extracts were concentrated, dissolved in water, and loaded onto a 1 g C18 solid-phase extraction column. Red pigment began to elute with 10% MeCN. The mobile phase was switched to 100% MeOH, and the combined eluate was concentrated in vacuo. The resulting residue was then purified by preparative HPLC using a Phenomenex Synergi 10 μm Hydro-RP 80, 250 × 21.2 mm preparative HPLC column (0–1 min isocratic 40% MeOH, 1–17 min 40%–65% MeOH; mobile phase buffered with 0.1% trifluoroacetic acid) to yield 6.4 mg. LC-MS and proton nuclear magnetic resonance (NMR) analysis matched ammosamide C, as reported previously by Hughes and Fenical (2010).

Production and Isolation of Compounds 4 and 8 from M512-pCAP01/*ammΔamm3* + pKY01/*amm3*

Both mutants, M512-pCAP01/*ammΔamm4* and M512-pCAP01/*ammΔamm3* + pKY01/*amm3*, produce compound **4**. However, for the isolation of **4**, we chose to use M512-pCAP01/*ammΔamm3* + pKY01/*amm3* due to consistently higher titers. Two 1 L cultures of M512-pCAP01/*ammΔamm3* + pKY01/*amm3* were grown for 12 days prior to centrifugation to remove cell debris. The resulting pink-colored supernatant could not be extracted with ethyl acetate or Amberlite XAD7HP resin. Thus, the entire 2 L was passed through a bed of C18 silica gel. The resulting bed was washed thoroughly with water and the pink pigments eluted with 10%–80% MeCN. The eluate was then lyophilized, and the resulting crude material was dissolved in 1:1 DMSO:MeOH for preparative HPLC purification with an Agilent Pursuit XRS 5 μm C18, 100 × 21.2 mm preparative HPLC column (0–1 min 5% MeCN isocratic, 1–25 min 5%–50% MeCN at 15 mL/min with a mobile phase buffered with 0.1% trifluoroacetic acid). See Supplemental Experimental Procedures for UV visible, HPLC, MS, and NMR spectra.

Compound **4** was further purified with on a Phenomenex Luna 5 μm C8(2) 250 × 100 mm semi-preparative column (0–20 min, 10%–13% MeCN at 4.5 mL/min with a mobile phase buffered with 0.1% trifluoroacetic acid) to yield 3.4 mg of **4**. ^{1}H-NMR (500 MHz, DMSO) δ 12.56 (s, 1H), 8.58 (s, 1H), 8.20 (s, 1H), 7.62 (s, 4H). ^{13}C-NMR (126 MHz, DMSO) δ 166.2, 148.8, 147.9, 147.2, 140.9, 138.3, 135.6, 132.5, 122.3, 119.4, 100.0. Exact mass calculated for **4** $[C_{11}H_7ClN_4O_2]H^+$ requires *m/z* = 263.0330, found 263.0356.

Compound **8** was further purified on a Phenomenex Luna 5 μm C8(2) 250 × 100 mm semi-preparative column (0–20 min, 15%–18% MeCN at 4.5 mL/min with a mobile phase buffered with 0.1% trifluoroacetic acid) to yield 0.8 mg of **8**. ^{1}H-NMR (599 MHz, DMSO) δ 10.20 (s, 1H), 8.32 (s, 1H), 6.57 (s, 2H), 6.37 (s, 2H). ^{13}C-NMR (126 MHz, DMSO) δ 166.1, 165.2, 140.7, 132.9, 132.3, 131.7, 120.6, 118.0, 105.0, 104.4. Exact mass calculated for **8** $[C_{11}H_7ClN_4O_3]H^+$ requires *m/z* = 279.0279, found 279.0314. The ^{1}H- and ^{13}C-NMR spectra matched synthetically prepared **8** (see Figure S5 and Supplemental Experimental Procedures).

Production and Isolation of Compounds 6 and 7 from M512-pCAP01/*ammΔamm23*

A 1 L culture of M512-pCAP01/*ammΔamm23* in R5 medium was extracted three times in ethyl acetate (3× 1 L), and the combined organics were dried with brine and anhydrous Mg_2SO_4 and then concentrated in vacuo. The resulting residue was then dissolved in 1:1 DMSO:MeOH and purified by preparative HPLC with an Agilent Pursuit XRS 5 C18 100 × 21.2 mm preparative HPLC column (0–1 min 5% MeCN isocratic, 1–20 min 5%–25% MeCN, at 15 mL/min with a mobile phase buffered with 0.1% trifluoroacetic acid). Both **6** and **7** were then further purified on a Phenomenex Luna 5 μm C8(2) 250 × 100 mm semi-preparative column (5%–25% MeCN at 4.5 mL/min with a mobile phase buffered with 0.1% trifluoroacetic acid) to yield 9.6 mg of **6** and 0.3 mg of **7**. See Supplemental Experimental Procedures for UV visible, HPLC, MS, and NMR spectra.

Compound **6** ^{1}H-NMR (500 MHz, DMSO) δ 8.93 (s, 1H), 8.80 (s, 1H), 8.54 (s, 1H), 7.75 (s, 1H). ^{13}C-NMR (126 MHz, DMSO) δ 165.9, 150.9, 148.3, 144.0, 136.9, 132.1, 128.3, 120.7, 119.6, 112.8, 98.4. Exact mass calculated for **6** $[C_{11}H_8ClN_5O]H^+$ requires *m/z* = 262.0490, found 262.0496.

Compound **7** ^{1}H-NMR (500 MHz, DMSO) δ 10.15 (s, 1H), 8.85 (s, 1H), 8.31 (s, 1H), 7.61 (s, 2H), 6.59 (s, 2H), 6.18 (s, 2H). ^{13}C NMR (126 MHz, DMSO) δ 166.3, 165.1, 144.5, 140.1, 131.7, 131.4, 131.1, 120.0, 115.5, 104.4, 103.7. Exact mass calculated for **7** $[C_{11}H_8N_5O_2]H^+$ requires *m/z* = 278.0439, found 278.0421. ^{1}H- and ^{13}C-NMR matched synthetic **7**. The ^{1}H- and ^{13}C-NMR spectra matched synthetically prepared **7** (see Figure S5, and Supplemental Experimental Procedures).

SUPPLEMENTAL INFORMATION

Supplemental Information includes Supplemental Experimental Procedures, five figures, and one table and can be found with this article online at http://dx.doi.org/10.1016/j.chembiol.2016.10.009.

AUTHOR CONTRIBUTIONS

P.A.J. conducted the experiments. P.A.J. and B.S.M. designed the experiments and wrote the manuscript.

ACKNOWLEDGMENTS

This work was funded by NIH grant R01-GM085770 to B.S.M. and an NIH postdoctoral fellowship to P.A.J. (5F32CA174333). Genome sequencing was conducted by the US Department of Energy Joint Genome Institute and supported by the Office of Science of the US Department of Energy under Contract No. DE-AC02-05CH11231. We thank our UCSD colleagues P.R. Jensen and W. Fenical for providing *Streptomyces* sp. CNR-698, C.C. Hughes for providing authentic standards, and B.M. Duggan and A.A. Mrse for providing NMR assistance. We are grateful for the helpful assistance from K. Yamanaka, E.N. Fielding, and K. Chang.

Received: July 2, 2016
Revised: September 9, 2016
Accepted: October 20, 2016
Published: November 17, 2016

REFERENCES

Altschul, S.F., Gish, W., Miller, W., Myers, E.W., and Lipman, D.J. (1990). Basic local alignment search tool. J. Mol. Biol. *215*, 403–410.

Antunes, E.M., Copp, B.R., Davies-Coleman, M.T., and Samaai, T. (2005). Pyrroloiminoquinone and related metabolites from marine sponges. Nat. Prod. Rep. *22*, 62–72.

Arnison, P.G., Bibb, M.J., Bierbaum, G., Bowers, A.A., Bugni, T.S., Bulaj, G., Camarero, J.A., Campopiano, D.J., Challis, G.L., Clardy, J., et al. (2013). Ribosomally synthesized and post-translationally modified peptide natural products: overview and recommendations for a universal nomenclature. Nat. Prod. Rep. *30*, 108–160.

Bentley, S.D., Chater, K.F., Cerdeno-Tarraga, A.M., Challis, G.L., Thomson, N.R., James, K.D., Harris, D.E., Quail, M.A., Kieser, H., Harper, D., et al. (2002). Complete genome sequence of the model actinomycete *Streptomyces coelicolor* A3(2). Nature *417*, 141–147.

Boddy, C.N. (2014). Bioinformatics tools for genome mining of polyketide and non-ribosomal peptides. J. Ind. Microbiol. Biotechnol. *41*, 443–450.

Boratyn, G.M., Camacho, C., Cooper, P.S., Coulouris, G., Fong, A., Ma, N., Madden, T.L., Matten, W.T., McGinnis, S.D., Merezhuk, Y., et al. (2013). BLAST: a more efficient report with usability improvements. Nucleic Acids Res. *41*, W29–W33.

Challis, G.L. (2008). Genome mining for novel natural product discovery. J. Med. Chem. *51*, 2618–2628.

Chatterjee, C., Paul, M., Xie, L., and van der Donk, W.A. (2005). Biosynthesis and mode of action of lantibiotics. Chem. Rev. *105*, 633–684.

Cimermancic, P., Medema, M.H., Claesen, J., Kurita, K., Brown, W., Laura, C., Mavrommatis, K., Pati, A., Godfrey, P.A., Koehrsen, M., et al. (2014). Insights into secondary metabolism from a global analysis of prokaryotic biosynthetic gene clusters. Cell *158*, 412–421.

Corre, C., and Challis, G.L. (2009). New natural product biosynthetic chemistry discovered by genome mining. Nat. Prod. Rep. *26*, 977–986.

Foulston, L.C., and Bibb, M.J. (2010). Microbisporicin gene cluster reveals unusual features of lantibiotic biosynthesis in actinomycetes. Proc. Natl. Acad. Sci. USA *107*, 13461–13466.

Geer, L.Y., Domrachev, M., Lipman, D.J., and Bryant, S.H. (2002). CDART: protein homology by domain architecture. Genome Res. *12*, 1619–1623.

Gomez-Escribano, J.P., and Bibb, M.J. (2012). *Streptomyces coelicolor* as an expression host for heterologous gene clusters. Methods Enzymol. *517*, 279–300.

Gomez-Escribano, J.P., and Bibb, M.J. (2014). Heterologous expression of natural product biosynthetic gene clusters in *Streptomyces coelicolor*: from genome mining to manipulation of biosynthetic pathways. J. Ind. Microbiol. Biotechnol. *41*, 425–431.

Goto, Y., Ito, Y., Kato, Y., Tsunoda, S., and Suga, H. (2014). One-pot synthesis of azoline-containing peptides in a cell-free translation system integrated with a posttranslational cyclodehydratase. Chem. Biol. *21*, 766–774.

Greening, C., Ahmed, F.H., Mohamed, A.E., Lee, B.M., Pandey, G., Warden, A.C., Scott, C., Oakeshott, J.G., Taylor, M.C., and Jackson, C.J. (2016). Physiology, biochemistry, and applications of F-420- and F-o-dependent redox reactions. Microbiol. Mol. Biol. Rev. *80*, 451–493.

Gust, B., Challis, G.L., Fowler, K., Kieser, T., and Chater, K.F. (2003). PCR-targeted *Streptomyces* gene replacement identifies a protein domain needed for biosynthesis of the sesquiterpene soil odor geosmin. Proc. Natl. Acad. Sci. USA *100*, 1541–1546.

Hentschel, U., Piel, J., Degnan, S.M., and Taylor, M.W. (2012). Genomic insights into the marine sponge microbiome. Nat. Rev. Micro. *10*, 641–654.

Hu, J.-F., Fan, H., Xiong, J., and Wu, S.-B. (2011). Discorhabdins and pyrroliminoquinone-related alkaloids. Chem. Rev. *111*, 5465–5491.

Hughes, C.C., and Fenical, W. (2010). Total synthesis of the ammosamides. J. Am. Chem. Soc. *132*, 2528–2529.

Hughes, C.C., MacMillan, J.B., Gaudencio, S.R., Jensen, P.R., and Fenical, W. (2009). The ammosamides: structures of cell cycle modulators from a marine-derived *Streptomyces* species. Angew. Chem. Int. Ed. Engl. *48*, 725–727.

Khusainov, R., and Kuipers, O.P. (2012). When the leader gets loose: in vivo biosynthesis of a leaderless prenisin is stimulated by a trans-acting leader peptide. ChemBioChem *13*, 2433–2438.

Kieser, T., Bibb, M.J., Buttner, M.J., Chater, K.F., and David, A.H. (2000). Practical *Streptomyces* Genetics (John Innes Foundation).

Koehnke, J., Mann, G., Bent, A.F., Ludewig, H., Shirran, S., Botting, C., Lebl, T., Houssen, W.E., Jaspars, M., and Naismith, J.H. (2015). Structural analysis of leader peptide binding enables leader-free cyanobactin processing. Nat. Chem. Biol. *11*, 558–563.

Kulathila, R., Merkler, K.A., and Merkler, D.J. (1999). Enzymatic formation of C-terminal amides. Nat. Prod. Rep. *16*, 145–154.

Li, C., and Kelly, W.L. (2010). Recent advances in thiopeptide antibiotic biosynthesis. Nat. Prod. Rep. *27*, 153–164.

McAuliffe, O., O'Keeffe, T., Hill, C., and Ross, R.P. (2001). Regulation of immunity to the two-component lantibiotic, lacticin 3147, by the transcriptional repressor LtnR. Mol. Microbiol. *39*, 982–993.

Merkler, D.J., Glufke, U., Ritenour-Rodgers, K.J., Baumgart, L.E., DeBlassio, J.L., Merkler, K.A., and Vederas, J.C. (1999). Formation of nicotinamide from nicotinuric acid by peptidylglycine alpha-amidating monooxygenase (PAM): a possible alternative route from nicotinic acid (niacin) to NADP in mammals. J. Am. Chem. Soc. *121*, 4904–4905.

Miyanaga, A., Janso, J.E., McDonald, L., He, M., Liu, H., Barbieri, L., Eustaquio, A.S., Fielding, E.N., Carter, G.T., Jensen, P.R., et al. (2011). Discovery and assembly-line biosynthesis of the lymphostin pyrroloquinoline alkaloid family of mTOR inhibitors in *Salinispora* bacteria. J. Am. Chem. Soc. *133*, 13311–13313.

Oman, T.J., and van der Donk, W.A. (2010). Follow the leader: the use of leader peptides to guide natural product biosynthesis. Nat. Chem. Biol. *6*, 9–18.

Oman, T.J., Knerr, P.J., Bindman, N.A., Velásquez, J.E., and van der Donk, W.A. (2012). An engineered lantibiotic synthetase that does not require a leader peptide on its substrate. J. Am. Chem. Soc. *134*, 6952–6955.

Ortega, M.A., Hao, Y., Zhang, Q., Walker, M.C., van der Donk, W.A., and Nair, S.K. (2015). Structure and mechanism of the tRNA-dependent lantibiotic dehydratase NisB. Nature *517*, 509–512.

Pan, E., Oswald, N.W., Legako, A.G., Life, J.M., Posner, B.A., and MacMillan, J.B. (2013). Precursor-directed generation of amidine containing ammosamide analogs: ammosamides E-P. Chem. Sci. *4*, 482–488.

Prigge, S.T., Kolhekar, A.S., Eipper, B.A., Mains, R.E., and Amzel, L.M. (1997). Amidation of bioactive peptides: the structure of peptidylglycine alpha-hydroxylating monooxygenase. Science *278*, 1300–1305.

Selengut, J.D., and Haft, D.H. (2010). Unexpected abundance of coenzyme F-420-dependent enzymes in *Mycobacterium tuberculosis* and other actinobacteria. J. Bacteriol. *192*, 5788–5798.

Silakowski, B., Schairer, H.U., Ehret, H., Kunze, B., Weinig, S., Nordsiek, G., Brandt, P., Blocker, H., Hofle, G., Beyer, S., et al. (1999). New lessons of combinatorial biosynthesis from myxobacteria – the myxothiazol biosynthetic gene cluster of *Stigmatella aurantiaca* DW4/3-1. J. Biol. Chem. *274*, 37391–37399.

Tang, X., Li, J., Millán-Aguiñaga, N., Zhang, J.J., O'Neill, E.C., Ugalde, J.A., Jensen, P.R., Mantovani, S.M., and Moore, B.S. (2015). Identification of thiotetronic acid antibiotic biosynthetic pathways by target-directed genome mining. ACS Chem. Biol. *10*, 2841–2849.

Udwary, D.W., Zeigler, L., Asolkar, R.N., Singan, V., Lapidus, A., Fenical, W., Jensen, P.R., and Moore, B.S. (2007). Genome sequencing reveals complex secondary metabolome in the marine actinomycete *Salinispora tropica*. Proc. Natl. Acad. Sci. USA *104*, 10376–10381.

van der Meer, J.R., Rollema, H.S., Siezen, R.J., Beerthuyzen, M.M., Kuipers, O.P., and de Vos, W.M. (1994). Influence of amino acid substitutions in the nisin leader peptide on biosynthesis and secretion of nisin by *Lactococcus lactis*. J. Biol. Chem. *269*, 3555–3562.

Volz, C., Kegler, C., and Müller, R. (2012). Enhancer binding proteins act as hetero-oligomers and link secondary metabolite production to myxococcal development, motility, and predation. Chem. Biol. *19*, 1447–1459.

Walsh, C. (1986). Naturally occurring 5-deazaflavin coenzymes – biological redox roles. Acc. Chem. Res. *19*, 216–221.

Walsh, C.T., and Fischbach, M.A. (2010). Natural products version 2.0: connecting genes to molecules. J. Am. Chem. Soc. *132*, 2469–2493.

Wang, P., Bashiri, G., Gao, X., Sawaya, M.R., and Tang, Y. (2013). Uncovering the enzymes that catalyze the final steps in oxytetracycline biosynthesis. J. Am. Chem. Soc. *135*, 7138–7141.

Weber, T. (2014). In silico tools for the analysis of antibiotic biosynthetic pathways. Int. J. Med. Microbiol. *304*, 230–235.

Weber, T., Blin, K., Duddela, S., Krug, D., Kim, H.U., Bruccoleri, R., Lee, S.Y., Fischbach, M.A., Müller, R., Wohlleben, W., et al. (2015). antiSMASH 3.0—a comprehensive resource for the genome mining of biosynthetic gene clusters. Nucleic Acids Res. *43*, W237–W243.

Yamanaka, K., Ryan, K.S., Gulder, T.A.M., Hughes, C.C., and Moore, B.S. (2012). Flavoenzyme-catalyzed atropo-selective N,C-bipyrrole homocoupling in marinopyrrole biosynthesis. J. Am. Chem. Soc. *134*, 12434–12437.

Yamanaka, K., Reynolds, K.A., Kersten, R.D., Ryan, K.S., Gonzalez, D.J., Nizet, V., Dorrestein, P.C., and Moore, B.S. (2014). Direct cloning and refactoring of a silent lipopeptide biosynthetic gene cluster yields the antibiotic taromycin A. Proc. Natl. Acad. Sci. USA *111*, 1957–1962.

Yeh, E., Garneau, S., and Walsh, C.T. (2005). Robust in vitro activity of RebF and RebH, a two-component reductase/halogenase, generating 7-chlorotryptophan during rebeccamycin biosynthesis. Proc. Natl. Acad. Sci. USA *102*, 3960–3965.

Zarins-Tutt, J.S., Barberi, T.T., Gao, H., Mearns-Spragg, A., Zhang, L., Newman, D.J., and Goss, R.J.M. (2015). Prospecting for new bacterial metabolites: a glossary of approaches for inducing, activating and upregulating the biosynthesis of bacterial cryptic or silent natural products. Nat. Prod. Rep. *33*, 54–72.

Zehner, S., Kotzsch, A., Bister, B., Sussmuth, R.D., Mendez, C., Salas, J.A., and van Pee, K.-H. (2005). A regioselective tryptophan 5-halogenase is involved in pyrroindomycin biosynthesis in *Streptomyces rugosporus* LL-42D005. Chem. Biol. *12*, 445–452.

Zeng, J., and Zhan, J. (2011). Characterization of a tryptophan 6-halogenase from *Streptomyces toxytricini*. Biotechnol. Lett. *33*, 1607–1613.

Zhang, Q., Yu, Y., Vélasquez, J.E., and van der Donk, W.A. (2012). Evolution of lanthipeptide synthetases. Proc. Natl. Acad. Sci. USA *109*, 18361–18366.

Ziemert, N., Alanjary, M., and Weber, T. (2016). The evolution of genome mining in microbes – a review. Nat. Prod. Rep. *33*, 988–1005.